Steady atomic entanglement in cavity QED without state initialization

ShengLi Zhang,[1,2] XuBo Zou,[1] Song Yang,[1] ChuanFeng Li,[1] ChenHui Jin,[2] and GuangCan Guo[1]

[1]*Key Laboratory of Quantum Information, University of Science and Technology of China (CAS), Hefei 230026, China*

[2]*Electronic Technology Institute, Information Engineering University, Zhengzhou, Henan 450004, China*

We present a scheme for realizing a steady entanglement state between two trapped atoms, without requiring the initialization of atom-cavity system nor fine time-controlling of evolution dynamics. We show that high-fidelity entanglement of atomic state can be obtained in a period of time equal to a few times the inverse of atomic's spontaneous decay rate. The robustness against cavity decay κ and cavity thermal field n_T has also been examined.

I. INTRODUCTION

Quantum entanglement states are a key ingredient for studying fundamental questions of quantum mechanics [1] and are considered to be a promising candidate for realizing distributed quantum computation and quantum information protocols [2,3]. In literature, a variety of schemes have been proposed to prepare atomic entanglement states with cavity QED systems. Based on their operating principle, these schemes can be generally divided as follows: (1) coherent evolution. This is one of the most common methods in quantum information processing. To create the entangling interactions between two distant atoms, it is straightforward to couple these atoms with a common medium, for example, the electromagnetic field or the resonator cavities, and then evolves them coherently. By fine time-controlling of the dynamics, the entanglement of the atoms can be obtained at a fixed time [4–8]. (2) Measurement induced entanglement. An alternative strategy is to employ the quantum measurement to enhance the two-atom entangling. For example, in Refs. [9–13], it was shown that the engineering of entanglement can also be probabilistically achieved by detecting the spontaneous or cavity decay photon through the single photon detectors. Moreover, entanglement of the internal levels of atoms can also be associated with the single photon polarization detection [14] and also with the balanced-homodyne detection [15]. (3) Macroscopic quantum jump. The underlying concept of macroscopic jump and entanglement state generation is quite interesting and relies on continuously monitoring of the macroscopic fluorescence signal leaking out of the cavity. Due to the conditional dynamics evolution, the monitoring detector will see long periods of fluorescence randomly interrupted by long periods of no fluorescence. The desired entanglement pure state can be created when no fluorescence is observed [16–18].

Beyond all those categories listed above, recently, there is a conceptually different approach—*steady entanglement* [19,20]. By utilizing lasers and cavity fields to drive two separate Raman transitions between the stable atomic ground state, Parkins showed that, in the limit of infinite large state squeezing, a maximally entangled steady state can be achieved. This relaxes the crucial requirement of fine time-controlling of coherent evolution or high-efficient quantum measurement.

In this paper, we propose an alternative method for generating steady entanglement between two trapped atoms.

However, comparing with the scheme proposed by Parkins and co-workers [19,20], our scheme has the following favorite features: (1) our scheme permits the unconditional preparation of entanglement state, which relieves the stringent requirement of atom state initialization as well as cavity initialization process. The initial state of the atomic-cavity system can be arbitrarily chosen, which is originally modeled with the Kronecker product of completely mixed state and thermal cavity state in this work. However, in Refs. [19,20], the initial state having no projection on antisymmetric subspace is a prerequisite condition. (2) The entanglement state provided here is in principle *pure* state. Moreover, the entanglement fidelity here shows an especially strong robustness against the cavity decay rate even in full Hamiltonian simulations.

This paper is organized as follows. In Sec. II, we present our model of atom-cavity system and evolution equations. In Sec. III, we use the effective Hamiltonian to evaluate the velocity at which the entanglement state is prepared. Section IV is devoted to entanglement state preparation under full Hamiltonian equation. The robustness against cavity decay κ and thermal field n_T has also been examined. The conclusions are drawn in Sec. V.

II. MODEL AND EFFECTIVE HAMILTONIAN

We here consider that two three-level atoms are tightly confined inside an optical cavity. These atoms are separated by such a large distance that the dipole-dipole interaction between these atoms can be ignored. The energy level configuration of the atoms is depicted in Fig. 1. It includes two stable ground states $|0\rangle, |1\rangle$ and one excited state $|2\rangle$. The
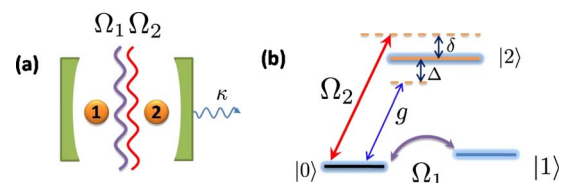
FIG. 1. (Color online) (a) Experimental setup consisting of two trapped atoms and a dispersive cavity. (b) Level structure for each atom. The atomic transition is nonresonantly coupled to the cavity mode a, while atomic transition $|0\rangle \leftrightarrow |1\rangle, |0\rangle \leftrightarrow |2\rangle$ are driven by two classic fields with Rabi frequency Ω_1, Ω_2.

transition $|0\rangle \leftrightarrow |1\rangle$ is coupled with a classic field (with Rabi frequency Ω_1), whereas the transition $|0\rangle \leftrightarrow |2\rangle$ is driven by both detuned laser field (with Rabi frequency Ω_2) and the cavity field (with cavity mode a). For simplicity, we assume that both atoms couple to the cavity mode with the same coupling strength g. Furthermore, all the coupling parameter g, Ω_1, Ω_2 is assumed to be real quantities for ease. Hereafter, we use ω_i to denote the Bohr frequency corresponding to the atomic transition $|0\rangle \leftrightarrow |i\rangle (i \in \{1,2\})$ and ω_f to denote the frequency of a single cavity mode. By using the subscript j to refer to the atom number, the master equation for the total system evolution can be given by

$$\dot{\rho} = -i[\mathcal{H}, \rho] + \sum_i \mathcal{L}[R_i], \qquad (1)$$

where $\mathcal{H} = \mathcal{H}_{\text{cav}} + \mathcal{H}_{\text{atom}} + \mathcal{H}_{\text{int}}$, with

$$\mathcal{H}_{\text{cav}} = \hbar \omega_f a^\dagger a, \qquad (2)$$

$$\mathcal{H}_{\text{atom}} = \hbar \omega_1 \sum_{j=1}^{2} |1\rangle_j \langle 1| + \hbar \omega_2 \sum_{j=1}^{2} |2\rangle_j \langle 2| + \hbar \Omega_1 \sum_{j=1}^{2} (e^{-i\omega_1 t} |1\rangle_j \langle 0|$$
$$+ \text{H.c.}) + \hbar \Omega_2 \sum_{j=1}^{2} (e^{-i(\omega_2 + \delta)t} |2\rangle_j \langle 0| + \text{H.c.}), \qquad (3)$$

$$\mathcal{H}_{\text{int}} = \hbar g \sum_{j=1}^{2} (a^\dagger |0\rangle_j \langle 2| + a|2\rangle_j \langle 0|), \qquad (4)$$

and H.c. denoting Hermitian conjugate.

The sum $\Sigma_i \mathcal{L}[R_i]$ represents all the possible relaxation channels, with each of which described by a Lindblad superoperator $\mathcal{L}[R_i] = \frac{1}{2}(2R_i \rho R_i^\dagger - R_i^\dagger R_i \rho - \rho R_i^\dagger R_i)$. Since the system can relax through the cavity decay and four spontaneous emission channels, we here need to consider five independent jump operators: $R_1 = \sqrt{\gamma_0}|0\rangle_1 \langle 2|$, $R_2 = \sqrt{\gamma_0}|0\rangle_2 \langle 2|$, $R_3 = \sqrt{\gamma_1}|1\rangle_1 \langle 2|$, $R_4 = \sqrt{\gamma_1}|1\rangle_2 \langle 2|$, and $R_c = \sqrt{\kappa}a$, with κ denoting the cavity decay rate and $\gamma_j (j = 0,1)$ representing the probability of atom's spontaneous transition $|2\rangle \rightarrow |j\rangle$. Although the jump operators are local operators, they can be used to generate the quantum entanglement. To see this, in the following, we will apply the Rotating Wave Approximation (RWA) [21,22] and adiabatically elimination to derive the effective performance of the system evolution.

We are particularly interested in the case where the light fields are largely detuned from the excited atomic states (i.e., $|\Delta = \omega_2 - \omega_f| \gg g, \Omega_1, \Omega_2, \gamma_0, \gamma_1$). We have applied the RWA twice to derive the effective Hamiltonian. First, taking account of $\Delta \gg g$, one can reduce the full Hamiltonian in Eq. (1) to

$$\mathcal{H} = \frac{g^2}{\Delta}(2|s_{02}\rangle \langle s_{02}| + |s_{12}\rangle \langle s_{12}| + |a_{12}\rangle \langle a_{12} + 2|22\rangle \langle 22|)$$
$$+ \Omega_1(\sqrt{2}|s_{01}\rangle \langle 00| + \sqrt{2}|s_{01}\rangle \langle 11| + |s_{02}\rangle \langle s_{12}| + |a_{02}\rangle \langle a_{12}|$$
$$+ \text{H.c.}) + \Omega_2[(|s_{01}\rangle \langle s_{12}| - |a_{01}\rangle \langle a_{12}| + \sqrt{2}|s_{02}\rangle \langle 22|$$
$$+ \sqrt{2}|00\rangle \langle s_{02}|)e^{i\delta t} + \text{H.c.}], \qquad (5)$$

in which we introduce the notation of symmetric basis $|s_{jk}\rangle$

$= (|kj\rangle + |jk\rangle)/\sqrt{2}$ and antisymmetric basis $|a_{jk}\rangle = (|kj\rangle - |jk\rangle)/\sqrt{2}$. Second, in Eq. (5), if g^2/Δ is much larger than Rabi frequency: $g^2/\Delta \gg \Omega_1, \Omega_2, \gamma_0, \gamma_1$, we can use the RWA again to eliminate the fast rotating items. Finally, the effective Hamiltonian of our system can be described by

$$\mathcal{H}_{\text{eff}} = i\varpi_1(|s_{01}\rangle \langle 00| + |s_{01}\rangle \langle 11| + \text{H.c.}) + i\varpi_2(|00\rangle \langle s_{02}| + |s_{02}\rangle$$
$$\times \langle 00|) + \Delta_{1E}[|s_{02}\rangle \langle s_{02}| + |a_{12}\rangle \langle a_{12}| - |s_{12}\rangle \langle s_{12}| - |a_{02}\rangle$$
$$\times \langle a_{02}|] + \sqrt{\Delta_{1E}\Delta_{2E}}[|s_{02}\rangle \langle s_{01}| + |s_{01}\rangle \langle s_{02}|] + \Delta_{2E}[|s_{01}\rangle$$
$$\times \langle s_{01}| + |a_{01}\rangle \langle a_{01}| - |s_{12}\rangle \langle s_{12}| - |a_{12}\rangle \langle a_{12}| + |s_{02}\rangle \langle s_{02}|$$
$$- |22\rangle \langle 22|], \qquad (6)$$

in which we have defined $\varpi_{1,2} = -i\sqrt{2}\Omega_{1,2}$, $\Delta_{1E,2E} = \Delta\Omega_{1,2}^2/g^2$.

The derivation of Eq. (6) also requires that the detuning $\delta = 2g^2/\Delta$. Namely, the basis state $|00\rangle$ must be "resonant" with the excited state $|s_{02}\rangle$. This is the most important guarantee that the steady entanglement state will be prepared effectively. Indeed, it can be easily observed that with such a kind of parameter configuration, state $|a_{01}\rangle$ happens to be the dark state of effective Hamiltonian $\mathcal{H}_{\text{eff}}$ and the system will fall to the steady state $|a_{01}\rangle$, eventually. It should also be noted that the items of cavity decay κ are automatically eliminated, which is a demonstration of the fact that our scheme is strongly robust against the cavity loss rate (See Fig. 3 for more information.)

III. ENTANGLEMENT GENERATION VELOCITY

As an important resource in quantum computation, entanglement state should not only be prepared with an ultra-high fidelity, but also the whole process should be completed within quite a short period of time. In the following, we will characterize the velocity at which the atom-cavity system evolves to the steady entangled state. For ease, we will study the dynamics evolution with the effective Hamiltonian, i.e.,

$$\dot{\rho_{AB}} = -i[\mathcal{H}_{\text{Eff}}, \rho] + \sum_{i=1}^{4} \mathcal{L}[R_i]. \qquad (7)$$

The initial state of the atomic state can be chosen arbitrarily. Without loss of generality, we assume that the atoms are populated in a mixed state

$$\rho_{AB}(0) = (|00\rangle \langle 00| + |01\rangle \langle 01| + |10\rangle \langle 10| + |11\rangle \langle 11|)/4. \qquad (8)$$

With the effective Hamiltonian equation (6), the effective equation of motion (7) is unchanged when exchanging the Hilbert Space of atom A and B. Exploring this property of commutable symmetry, the evolution $\dot{\rho_{AB}}$ can be further simplified to an evolution confined in a five-dimensional subspace.

We rewrite the derivative of density matrix $\dot{\rho_{AB}}$ in the basis $|e_0\rangle = |a_{01}\rangle$, $|e_1\rangle = |s_{01}\rangle$, $|e_2\rangle = |s_{02}\rangle$, $|e_3\rangle = |00\rangle$, $|e_4\rangle = |11\rangle$, $|e_5\rangle = |a_{02}\rangle$, $|e_6\rangle = |a_{12}\rangle$, $|e_7\rangle = |s_{12}\rangle$, $|e_8\rangle = |22\rangle$. It can be easily checked that all the nonzero matrix entries $\langle e_i|\rho_{AB}(t)|e_j\rangle$ are restricted in the $\{|e_0\rangle, |e_1\rangle, |e_2\rangle, |e_3\rangle, |e_4\rangle\}$ subspace and what is more important is that in this subspace
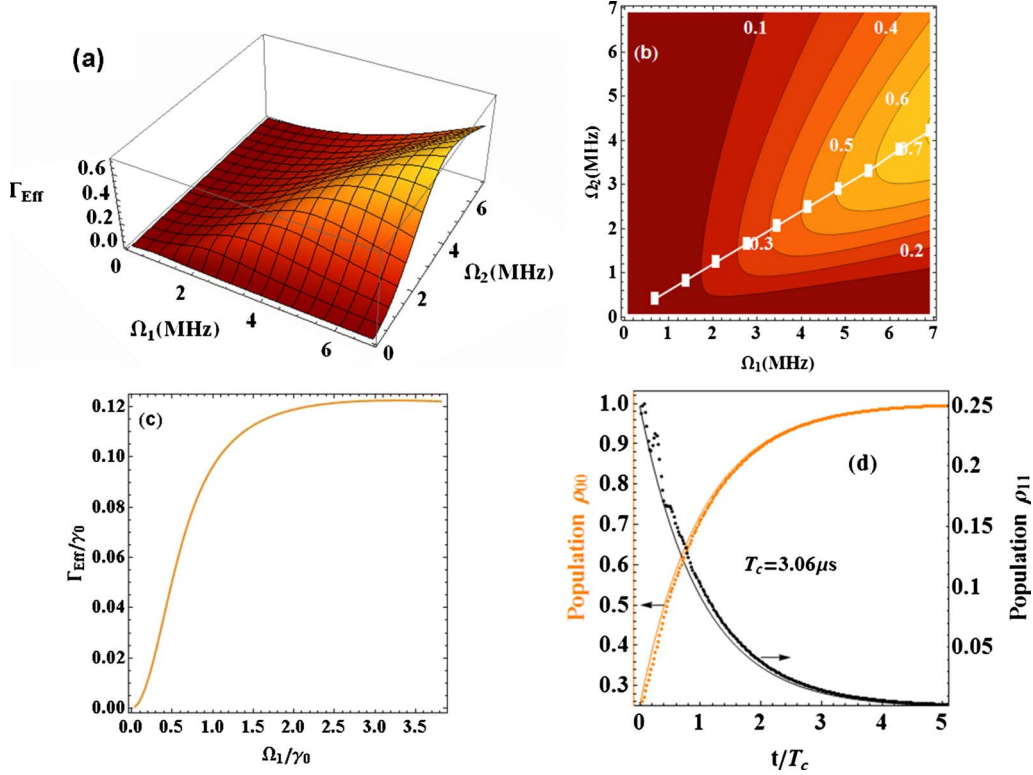
FIG. 2. (Color online)(a) The effective Γ_{Eff} at which our system approaches the steady state. (b) Contour plot of the Γ_{Eff}. The line $\Omega_2 = 3\Omega_1/5$ indicates the stationary points where the optimization is achieved. Other parameters are set according to the typical experiment values $(g, \kappa, \Delta, 2\gamma_0, 2\gamma_1)/2\pi = (110, 14.2, 800, 2.6, 2.6)$ MHz. (c) Γ_{Eff} as a function of Rabi frequency Ω_1/γ_0 ($\Omega_2 = 3\Omega_1/5$ satisfied). (d) State evolution under simplified Hamiltonian equation (9). The solid lines show the exponential variation in population $\rho_{00}, \rho_{11} \equiv \langle e_1 | \rho | e_1 \rangle$. The numerical simulation from direct integration of Eq. (9) is presented with the dotted lines. The parameters for both result are chosen as $\Omega_1 = 3.45$ MHz, $\Omega_2 = 2.14$ MHz, $2\gamma_0 = 2.6 \times 2\pi$ MHz, which leads to a characteristic time $T_c = \Gamma_{\text{Eff}}^{-1} = 3.06$ μs. The steady state entanglement with fidelity $F_{\text{atom}} = 0.9948$ is approached at $t \sim 5T_c$.

$\dot{\rho}_{00} \equiv \langle e_0 | \rho_{AB}(t) | e_0 \rangle$ is completely decoupled from $\langle e_i | \dot{\rho}_{AB}(t) | e_j \rangle (i, j = 1, 2, 3, 4)$. Therefore, one can seek a solution of the form $\rho_{AB}(t) = \tilde{\varrho}(t) + (1 - \text{Tr}[\tilde{\varrho}]) | a_{01} \rangle \langle a_{01} |$, in which $\tilde{\varrho}$ resides in the subspace of $\{|e_1\rangle, |e_2\rangle, |e_3\rangle, |e_4\rangle\}$ and satisfies

$$\frac{d\tilde{\varrho}}{dt} = \mathcal{M}\tilde{\varrho} + \tilde{\varrho}\mathcal{M}^\dagger + \mathcal{E}(\tilde{\varrho}), \qquad (9)$$

with

$$\mathcal{M} = \begin{pmatrix} 0 & \sqrt{\Delta_{1E}\Delta_{2E}} & \varpi_2 & \varpi_2 \\ \sqrt{\Delta_{1E}\Delta_{2E}} & \dfrac{\Gamma_0 + \Gamma_1}{2} & \varpi_1 & \varpi_1 \\ \varpi_2 & \varpi_1 & \Delta_{1E} & 0 \\ \varpi_2 & 0 & 0 & \Delta_{1E} \end{pmatrix} \qquad (10)$$

and [23]

$$\mathcal{E}(\tilde{\varrho}) = \begin{pmatrix} -\Gamma_1 \tilde{\rho}_{22}/2 & \Sigma_{12} & 0 & 0 \\ \Sigma_{12}^* & \varpi_1(\tilde{\rho}_{24} - \tilde{\rho}_{42}) & \Sigma_{23} & \Sigma_{24} \\ 0 & \Sigma_{23}^* & -\tilde{\rho}_{22}\Gamma_0 & 0 \\ 0 & \Sigma_{24}^* & 0 & 0 \end{pmatrix} \qquad (11)$$

written in term of basis $\{|e_1\rangle, |e_2\rangle, |e_3\rangle, |e_4\rangle\}$.

Then, we will resort to the vector formalization of the reduced equation (9). The method is very simple and straightforward: one simply constructs a 16-dimension vector $\vec{v}$ by taking the elements of density matrix $\tilde{\varrho}$ column-wisely. This helps to define a one-to-one correspondence between the arbitrary operation $\mathcal{A}$ acting on $\tilde{\varrho}$ and operator acting on $\vec{v}$

$$\mathcal{A}\tilde{\varrho} \leftrightarrow (\mathcal{I} \otimes \mathcal{A})\vec{v}, \quad \tilde{\varrho}A \leftrightarrow (\mathcal{A}^\tau \otimes \mathcal{I})\vec{v}, \qquad (12)$$

with $\mathcal{I}$ denoting a 4×4 unit matrix and τ denoting the matrix transpose. In this case, the evolution equation of $\dot{\tilde{\varrho}}$ can be rephrased as

$$\dot{\vec{v}} = X\vec{v}. \qquad (13)$$

All the 16 eigenvalues $\lambda_1, \lambda_2, \ldots, \lambda_{16}$ of X have a negative real part, which, in turn, drives our system to the final steady state. The entanglement generation velocity, namely, the time scale at which our system approaches steady state can be easily determined with the minimum of the absolute value of these real parts. By defining $\Gamma_{\text{Eff}} \equiv \min_{1 \le i \le 16} |\text{Re}(\lambda_i)|$, one can approximate the solution to Eq. (13) with $\vec{v} = \vec{v_0} e^{-t\Gamma_{\text{Eff}}}$, where $\vec{v_0}$ is the initial condition for the dynamics evolution [Eq. (13)]. For the mixed state Eq. (8), one obtains $\vec{v_0} = \frac{1}{4}(|e_1\rangle|e_1\rangle + |e_3\rangle|e_3\rangle + |e_4\rangle|e_4\rangle)$. For ease, in the following, we
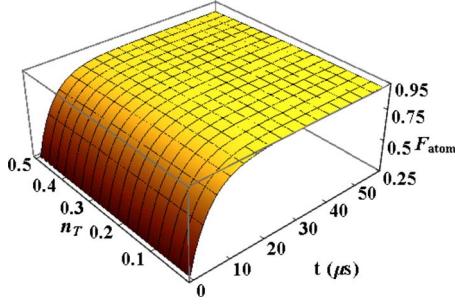
FIG. 3. (Color online) The fidelity of atomic entanglement as a two-variable function of evolving time t and average photon number in the cavity n_T. Other parameters such as $(g, \kappa, \Delta, \gamma_0, \gamma_1, \Omega_1, \Omega_2)$ are chosen from Fig. 2.

will also frequently use the characterization time $T_c = \Gamma_{\text{Eff}}^{-1}$ to evaluate the entanglement generation velocity.

In general, the eigenspectral decomposition of matrix X is very complicated, and in Fig. 2(a), we plot Γ_{Eff} as a function of the Rabi frequency Ω_1 and Ω_2. In fact, we have considered an example where Fabry-Perot cavity with cavity length $l = 10.6$ μm and cavity fitness $F = 4.8 \times 10^5$ is relevant [24]. We assume two cesium atoms are trapped in the standing-wave mode for maximal coupling, such that $(g, \kappa, 2\gamma_0, 2\gamma_1)/2\pi = (110, 14.2, 2.6, 2.6)$ MHz and atomic excited state detuning $\Delta/2\pi = 800$ MHz. Taking account of the large-detuning condition, we choose $\Omega_1(\Omega_2)$ varying from $0 \sim 6.6$ MHz. For $\Omega_1 = 3.45$ MHz, numerical optimization provides a maximal generation velocity $\Gamma_{\text{Eff}} = 0.33$ MHz at $\Omega_2 = 2.14$ MHz. Further detailed analysis gives the optimization condition $\Omega_2 = 3\Omega_1/5$, and a contour plot is also presented in Fig. 2(b). With such relation, we then consider the asymptotic limit of Γ_{Eff}. Figure 2(c) describes Γ_{Eff} as a function of the Rabi frequency Ω_1. For small Ω_1/γ_0, e.g., $0 < \Omega_1/\gamma_0 < 3$, Γ_{Eff} increases fast with Ω_1/γ_0. Further increasing Ω_1, the velocity of the increasing slows down, and in the large limit $\Omega_1 \sim 10\gamma_0$, Γ_{Eff} ceases to increase obviously and approaches a value $\sim \gamma_0/8$. Finally, as a verification of the rate of entanglement generation, we numerically solve the state evolution equation (9) and plot the state population in Fig. 2(d). The characterization time is $T_c = \Gamma_{\text{Eff}}^{-1} = 3.06$ μs and the final state approaches the maximal entanglement steady state: $\rho_{00} = \langle a_{01}|\rho|a_{01}\rangle = 0.9948$ at $t \sim 5T_c$. The solid lines indicate the exponential variation in population: $\rho_{00} = 1 - 3e^{-\Gamma_{\text{Eff}}t}/4$ and $\rho_{11} = e^{-\Gamma_{\text{Eff}}t}/4$, which coincides very well with the numerical integration (shown with dotted lines).

IV. DYNAMICS OF ENTANGLEMENT UNDER FULL HAMILTONIAN

The effective Hamiltonian is found by adiabatically eliminating the cavity field, and of course our scheme shows an intrinsic robustness against the cavity decay κ. However, in practice, it is quite necessary to give a thorough study of the actual performance of our model. In the following, with no approximations, we investigate our atom-cavity system with the full Hamiltonian equation (1). Our investigation will be
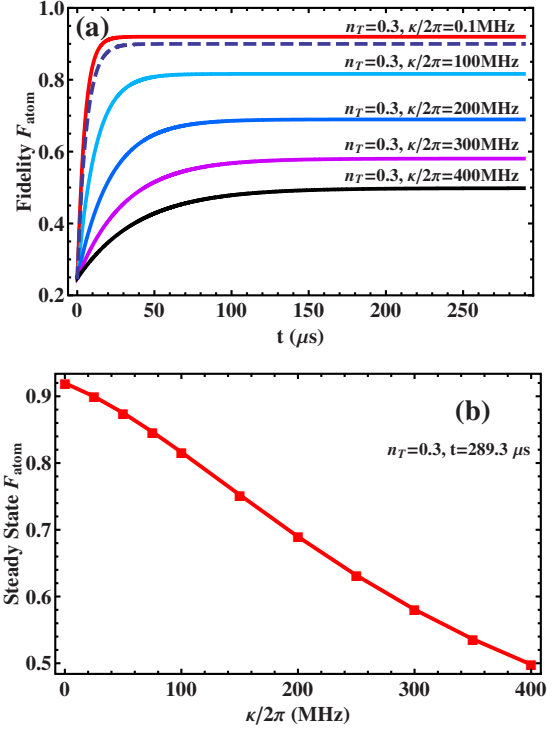
FIG. 4. (Color online) Cavity decay κ as an important factor that suppresses the atomic entanglement. For ease, we choose $n_T = 0.3$. All parameters $(g, \Delta, \gamma_0, \gamma_1, \Omega_1, \Omega_2)$ are identical with the ones in Fig. 2. (a)The atom-cavity system approaches the steady state at the time $t = 289.3$ μs, for large κ. Dashed line indicates the case of $\kappa/2\pi = 25$ MHz. (b) The steady entanglement fidelity as a Monotonously decreasing function of decay κ. When $\kappa/2\pi = 400$ MHz ~ 3.64 g, the entanglement fidelity is as low as 0.4981.

divided into four parts: first, we will discuss the robustness of entanglement against initial state. Second, the suppressing effect of the cavity decay κ will be characterized. Third, we will check the exact form of steady state under full Hamiltonian. As a comparison, the exact steady state of both effective Hamiltonian and full Hamiltonian is also presented. Finally, the limit and validity of the effective Hamiltonian is discussed.

First of all, we define the fidelity of atomic state as a quantitative measure of entanglement: $F_{\text{atom}} = \langle a_{01}|\rho_{AB}(t)|a_{01}\rangle$, where $\rho_{AB}(t)$ represents the temporal reduced density matrix obtained by tracing out the cavity mode.

A. Robustness of entanglement against initial state

Let us first investigate the dependence of entanglement upon the initial state of the atom-cavity system. In fact, our system can still work very well without cavity initialization or atomic state prepurification. To show this, both atom and cavity field are originally set in some mixed state and numerical integration of Eq. (1) is employed to describe their evolution. The mixed state we use is $\rho_{AB-\text{cav}}(0)$

$$\rho_{AB-\text{cav}}(0) = \rho_{AB}(0) \otimes \rho_T, \qquad (14)$$

with $\rho_T = \sum_{n=0}^{\infty} \frac{n_T^n}{(1+n_T)^{n+1}}|n\rangle\langle n|$ denoting the thermal state and $\rho_{AB}(0)$ defined in Eq. (8).
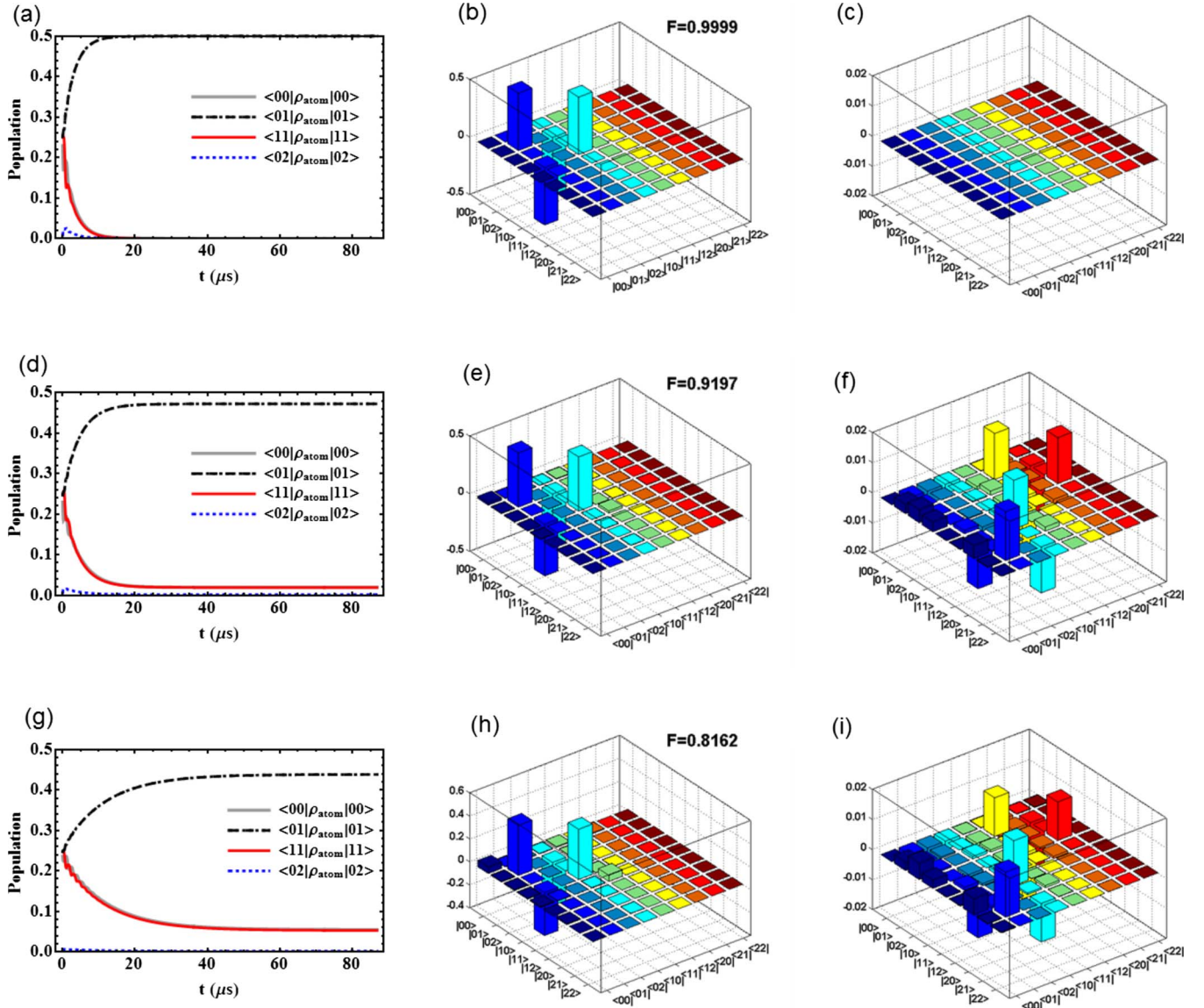
FIG. 5. (Color online) State population at steady state under effective Hamiltonian and full Hamiltonian, for $(g, \Delta, 2\gamma_0, 2\gamma_1, \Omega_1, \Omega_2)/2\pi = (110, 800, 2.6, 2.6, 0.54, 0.34)$ MHz. (a) State evolution derived from the effective Hamiltonian [Eq. (6)]. The characteristic time is still $T_c = 3.06$ μs and the whole system is definitely stabilized at $t = 28.93$ μs $\sim 9.45 T_c$. (b) and (c) are the real and imaginary parts of the atomic state ρ_{atom} for steady state in (a). (d) State evolution with full-model equation (1) for time $t : 0 \sim 86.79$ μs, $\kappa = 0.1$ MHz. (e) and (f) are the real and imaginary parts of corresponding steady state at $t = 86.79$ μs. (g) State evolution with full-model equation (1) and $\kappa = 100$ MHz, real and Imaginary parts of final state is shown in (h) and (i).

In Fig. 3, we plot the fidelity F_{atom} as a function of both cavity decay rate κ and thermal cavity field (characterized by the mean photon number n_T). The exact values of all parameters (except n_T) are chosen from Fig. 2. With a given average photon number n_T, the fidelity of atomic entanglement increases monotonically and quickly with the evolution time t. When time $t \sim 4 \times 10^4 / g = 57.86$ μs $\approx 19 T_c$, the fidelity ceases to increase, obviously, and the atom-cavity system approximates the steady state. The fidelity F_{atom} of entanglement at steady state shows little dependence on the average photon number n_T, which is a good proof of the robustness of our scheme.

B. Cavity decay κ as a suppressing factor

Here, we investigate the effect of κ on our scheme. Since our system is robust against initial state (as shown in Fig. 3), we set $n_T = 0.3$. In Fig. 4(a), we plot the dynamics evolution of the entanglement fidelity. At very long time, $t = 289.3$ μs, the state of the whole system is stabilized and then preserved. The cavity decay κ acts as an important factor that suppresses the final entanglement. When $\kappa = 25$ MHz $\ll g$, the entanglement fidelity is about 0.8997, as shown with the dashed line in Fig. 4(a). However, for a large κ, two salient effects are observed. (1) The fidelity significantly decreases with increasing κ. For example, when $\kappa = 400$ MGz

~ 3.64 g, the fidelity as low as 0.4981 is observed. More details of this monotonous decreasing property is depicted in Fig. 4(b). (2) The time when the systems fall to steady state is definitely influenced. For $\kappa = 25$ MHz, 30 μs is sufficient for evolution. Whereas for $\kappa = 400$ MHz, a long time of 200 μs is required. Of course, all these two results are somewhat different from the effective Hamiltonian based equation [Eq. (9)], which is κ independent. In the following, Sec. IV C, we will characterize what the exact steady state is and give a more detailed comparison of entanglement dynamics in two scenarios: with effective Hamiltonian and with full Hamiltonian.

C. Exact form of steady state in full Hamiltonian and effective Hamiltonian

As is shown in Fig. 4(a), once the atomic-cavity system falls to steady state, the state will be preserved, as long as the present Hamiltonian is not altered. In order to give a detailed description of the final state, we give a plot in Fig. 5.

(1) For effective Hamiltonian, as noted after Eq. (6), the singlet state $|a_{01}\rangle = \frac{1}{\sqrt{2}}(|01\rangle - |10\rangle)$ happens to be the dark state of our system. This can be more easily observed in Fig. 5(a). All the populations in symmetric state such as $\langle 00|\rho_{\text{atom}}|00\rangle, \langle 11|\rho_{\text{atom}}|11\rangle$ decay exponentially, whereas the population in $\langle 01|\rho_{\text{atom}}|01\rangle$ increases monotonously. The density matrix of the final steady state at $t = 86.79$ μs is shown in (b) (real part) and (c) (imaginary part). The fidelity is as high as 0.9999 and no pronounced population at excited level $|2\rangle$ is observed.

(2) For full-model Hamiltonian and low κ, the fidelity of entanglement at a relatively high level is still observed. In Fig. 5(d), we plot the state population for the limiting case of $\kappa = 0.1$ MHz. At steady state, there exists a finite population at symmetric state: $\langle 11|\rho_{\text{atom}}|11\rangle = 0.0192$, $\langle 00|\rho_{\text{atom}}|00\rangle = 0.0195$, which certainly decrease the population at $|01\rangle$:$\langle 01|\rho_{\text{atom}}|01\rangle = 0.4721$. Finally, the entanglement fidelity is 0.9197. The real and imaginary part of the density matrix is shown in (e) and (f), respectively.

(3) Full Hamiltonian and very large κ. As shown in Sec. IV B, cavity decay κ is a suppressing factor for the fidelity of entanglement. We take $\kappa = 100$ MHz as an example and investigate the relevant steady states. The population is shown in Fig. 5(g) and the density matrix are shown in Fig. 5(h) (real part) and (i) (imaginary part). Comparing with Fig. 5(d), the population of steady state in symmetric state subspace increases, $\langle 11|\rho_{\text{atom}}|11\rangle = 0.0528$, $\langle 00|\rho_{\text{atom}}|00\rangle = 0.0546$. The fidelity $F = 0.8162$, however, shows obvious decrease. Moreover, the time required to achieve steady state is now prolonged to ~ 80 μs.

D. Limit of validity of Effective Hamiltonian

For completeness, it is now necessary to give some discussions of deviations between state evolution under effective Hamiltonian equation (7) and full Hamiltonian equation (1) and where these deviations come from.

First of all, to make the problem much more tractable, we neglect the effect of κ by considering a rather low decay case $\kappa = 0.1$ MHz $\sim 10^{-3}$ g. In Fig. 6(a), we show how these de-
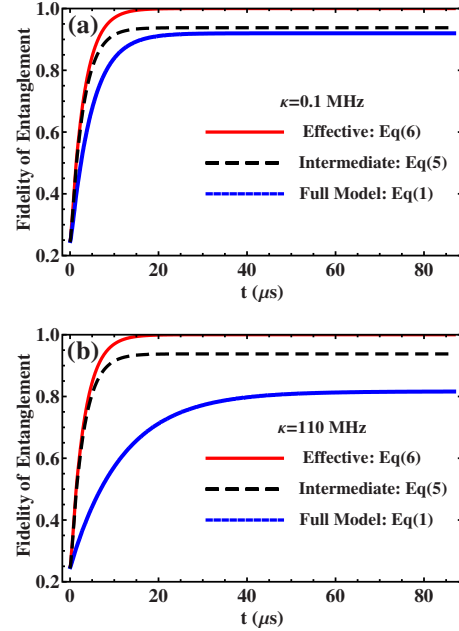
FIG. 6. (Color online) Fidelity of atomic entanglement F_{atom} under effective Hamiltonians (solid lines), intermediate Hamiltonian equation (5) (dashed lines), and full Hamiltonians (dotted lines). All parameters $(g, \Delta, \gamma_0, \gamma_1, \Omega_1, \Omega_2)$ are identical with the ones in Fig. 2. (a) $\kappa = 0.1$ MHz. (b) $\kappa = 100$ MHz.

viations is gradually introduced. The fidelity of atomic entanglement state derived from effective Hamiltonian is $F_{\text{eff}} = 0.9999$, whereas the fidelity derived from full-model equation (1) is $F_{\text{full}} = 0.9197$. Indeed, the loss of fidelity can be determined from the large-detuning approximations in Eqs. (5) and (6). To be more specific, we plot the state evolution with the intermediate Hamiltonian equation (5) and finally, the fidelity at steady state is $F_{\text{int}} = 0.9378$. Namely, the loss of fidelity $F_{\text{eff}} - F_{\text{int}} = 0.0621$ is introduced from the second large-detuning approximation $g^2/\Delta \gg \Omega_1, \Omega_2, \gamma_0, \gamma_1$. The further loss of fidelity $F_{\text{int}} - F_{\text{full}} = 0.0181$ is due to the first large-detuning approximation $|\Delta| \gg g, \kappa, \Omega_1, \Omega_2, \gamma_0, \gamma_1$. Moreover, the loss of velocity can be clearly observed in both Figs. 6(a) and 6(b). The evolution of effective Hamiltonian equation (6) (solid lines) and intermediate Hamiltonian equation (5) (dashed lines) shows the same velocity, while the evolution for full Hamiltonian equation (1) (dotted lines) is delayed. In our exemplary parameters for $(g, \kappa, \gamma_0, \gamma_1)$, the large-detuning relation is not well satisfied and that is the reason why final atomic state is not the maximal entanglement pure state.

Indeed, we also evaluate the same atom-cavity system, except that the atomic decay is set as $2\gamma_0 = 2\gamma_1 = 0.26 \times 2\pi$ MHz. In this case, one can see a remarked improvement in the entanglement state preparation and a high-fidelity $F = 0.9596$ can be achieved [25]. However, from the experimental point of view, this requires further suppression of spontaneous emission rate. Here, we remarked that such a problem may be solved by placing the atom near a reflecting plane or in the fabricated optical cavity, which has already been shown theoretically [26] as well as experimentally [27].

V. CONCLUSIONS

The scheme presented in this paper allows us to prepare steady entanglement of two three-level atoms, which are both trapped inside the same optical cavity. The scheme only requires two driving fields and can even work very well without cavity field initialization or atoms state prepurification. In our simulation, for example, the initial state of cavity field and atoms are assumed to be thermal state and mixed state, respectively. We believe this steady entanglement approach are of great physical interest and will have possible technological applications in quantum state engineering.

[1] J. S. Bell, Physics (Long Island City, N.Y.) **1**, 195 (1965).

[2] C. Monroe, Nature (London) **416**, 238 (2002).

[3] H. Mabuchi and A. C. Doherty, Science **298**, 1372 (2002).

[4] J. I. Cirac and P. Zoller, Phys. Rev. A **50**, R2799 (1994).

[5] E. Hagley, X. Maitre, G. Nogues, C. Wunderlich, M. Brune, J. M. Raimond, and S. Haroche, Phys. Rev. Lett. **79**, 1 (1997).

[6] M. Freyberger, P. K. Aravind, M. A. Horne, and A. Shimony, Phys. Rev. A **53**, 1232 (1996).

[7] B. J. Oliver and C. R. Stroud, J. Opt. Soc. Am. B **4**, 1426 (1987).

[8] I. K. Kudryavtsev and P. L. Knight, J. Mod. Opt. **40**, 1673 (1993).

[9] L. M. Duan and H. J. Kimble, Phys. Rev. Lett. **90**, 253601 (2003).

[10] S. Bose, P. L. Knight, M. B. Plenio, and V. Vedral, Phys. Rev. Lett. **83**, 5158 (1999).

[11] A. S. Sørensen and K. Mølmer, Phys. Rev. Lett. **90**, 127903 (2003).

[12] C. Cabrillo, J. I. Cirac, P. García-Fernández, and P. Zoller, Phys. Rev. A **59**, 1025 (1999).

[13] D. E. Browne, M. B. Plenio, and S. F. Huelga, Phys. Rev. Lett. **91**, 067901 (2003).

[14] J. Hong and H. W. Lee, Phys. Rev. Lett. **89**, 237901 (2002).

[15] A. S. Sørensen and K. Mølmer, Phys. Rev. Lett. **91**, 097905 (2003).

[16] J. Metz, M. Trupke, and A. Beige, Phys. Rev. Lett. **97**, 040503 (2006).

[17] J. Metz and A. Beige, Phys. Rev. A **76**, 022331 (2007).

[18] M. B. Plenio, S. F. Huelga, A. Beige, and P. L. Knight, Phys. Rev. A **59**, 2468 (1999).

[19] S. G. Clark and A. S. Parkins, Phys. Rev. Lett. **90**, 047905 (2003).

[20] A. S. Parkins, E. Solano, and J. I. Cirac, Phys. Rev. Lett. **96**, 053602 (2006).

[21] D. F. V. James, Fortschr. Phys. **48**, 823 (2000).

[22] M. S. Zubairy, M. Kim, and M. O. Scully, Phys. Rev. A **68**, 033820 (2003).

[23] It can be directly obtained that $\Sigma_{12}=-\varpi_1\tilde{\varrho}_{14}-i\Delta_{2E}\tilde{\varrho}_{12}$, $\Sigma_{23}=\varpi_1\tilde{\varrho}_{43}+i\Delta_{2E}\tilde{\varrho}_{23}$, and $\Sigma_{24}=\varpi_1\tilde{\varrho}_{44}+i\Delta_{2E}\tilde{\varrho}_{24}$.

[24] C. J. Hood *et al.*, Science **287**, 1447 (2000).

[25] With a much lower γ, the characterization time will be prolonged, which may impose some limitation on the velocity for state preparation.

[26] D. Kleppner, Phys. Rev. Lett. **47**, 233 (1981); F. De Martini, G. Innocenti, G. R. Jacobovitz, and P. Mataloni, *ibid.* **59**, 2955 (1987); W. Jhe, A. Anderson, E. A. Hinds, D. Meschede, L. Moi, and S. Haroche, *ibid.* **58**, 666 (1987).

[27] T. J. Rogers, D. G. Deppe, and B. G. Streetman, Appl. Phys. Lett. **57**, 1858 (1990).